Tellus SERIES B CHEMICAL AND PHYSICAL METEOROLOGY
PUBLISHED BY THE INTERNATIONAL METEOROLOGICAL INSTITUTE IN STOCKHOLM

Short-term variability of total column ozone from the Dobson spectrophotometer measurements at Belsk, Poland, in the period 23 March 1963–31 December 2019

By J. W. KRZYŚCIN*, B. RAJEWSKA-WIĘCH, and J. BORKOWSKI, *Institute of Geophysics, Polish Academy of Science, Warsaw, Poland*

(Manuscript received 9 November 2020; in final form 1 April 2021)

ABSTRACT

Total column ozone (TCO) monitoring with the Dobson spectrophotometer no. 84 have been carried out at Belsk (51°50′, 20°47′), Poland, since 23 March 1963. TCO observations were made for various combinations of double wavelength pairs (AD, CD, CC′) and instrument settings (direct Sun, zenith blue, and zenith cloudy). In total, results of 115,736 manual observations were recorded in the period 1963–2019. The following metrics of the intraday TCO variability are examined: standard deviation divided by the mean value and the difference between the daily maximum and minimum divided by the mean value. The mean value, standard deviation, and 5th–95th percentile range for the intraday changes of the metrics are {1.6%, 0.8%, 2.5%} and {4.3%, 2.3%, 7.3%,}, respectively. To examine interday TCO variability, one-day changes of the metrics and the daily mean TCO are analysed. The corresponding statistics for one-day change of TCO are {−0.2%, 6.9%, 22.6%}. The short-term TCO variability changed only slightly (if ever) since the beginning of the ozone observations at Belsk.

Keywords: total column ozone, short-term variability, trends

1. Introduction

Anthropogenic changes in the stratospheric ozone layer have been the subject of scientific and public interest for almost half a century. The possible thinning of the ozone layer was suggested in the early 1970s by the 1995 laureates of the Noble Prize in Chemistry: Paul J. Crutzen, Mario J. Molina, and F. Sherwood Roland (Crutzen, 1971; Molina and Rowland, 1974). In the early 1980s, significant depletion of the ozone layer was found over Antarctica, i.e. the so-called ozone hole (Chubachi, 1984; Farman et al., 1985). The widespread interest in the ozone hole over Antarctica was due to the expected increase in the intensity of harmful ultraviolet (UV) radiation on the Earth's surface in Antarctica and possibly in other parts of the globe.

In response to the threat of ozone destruction, the Montreal Protocol (MP) was signed in 1987, which established restrictions on the production of the most ozone depleting substances (ODS) (e.g. chlorofluorocarbons – CFC) containing chlorine and bromine, which are involved in the catalytic destruction of the stratospheric ozone shield against the UV radiation. Ground-based monitoring of the ozone layer with Dobson spectrophotometers played a decisive role in the discovery of the Antarctic ozone hole and led to the identification (in the beginning of 1990s) of significant long-term ozone depletion in winter and spring over extratropical regions (Staehelin et al., 2018 and the references therein). Establishing a world standard for the Dobson instrument (Dobson spectrophotometer No. 83) was decisive for maintaining the high quality of the global Dobson network (Komhyr et al., 1989).

The MP implementation and its further amendments resulted in a turnaround of the ODS concentration in the stratosphere in the late 1990s (middle latitudes) and ~2000 (high latitudes) (WMO, 2018). Since then, an accompanying trend reversal (from negative to positive value) in total column ozone (TCO) should be identified.

*Corresponding author. email: jkrzys@igf.edu.pl

Citation: Tellus B: 2021, **73**, 1912958, https://doi.org/10.1080/16000889.2021.1912958

Determining the onset of ozone regeneration in response to ODS changes has been the subject of extensive scientific debate based on the results of the statistical and chemistry-climate models (Reinsel et al., 2005; Harris et al., 2008; Morgenstern et al., 2010; Dhomse et al., 2018; Krzyścin and Baranowski, 2019). Clear signs of the Antarctic ozone recovery have recently been revealed (Solomon et al., 2016; Pazmiño et. al., 2018; Kuttippurath et al., 2018; Krzyścin, 2020).

Surprisingly the ozone depletion still exists in the lower stratosphere in the Northern Hemisphere midlatitudes (Ball et al., 2018; Chipperfield et al., 2018) that is forced by dynamical effects. Unexpected signs of increasing contamination of the atmosphere by CFC have recently been revealed in eastern mainland China (Montzka et al., 2018; Rigby et al., 2019) suggesting that the protection of the ozone layer by the MP and its further amendments is not as effective as previously thought. Therefore, the problem of the stratospheric ozone depletion is still relevant and requires further research.

Usually, the ozone observations were averaged on the monthly basis and used in long-term variability studies. This paper is an extension of our earlier paper (Krzyścin et al., 2013) focusing solely on trends in the Belsk's TCO. We will discuss the short-term TCO variability using of the Belsk's intraday TCO data base (Rajewska-Więch et al., 2020). The following daily metrics characterising short-term TCO variability are considered, coefficient of variability (CV) (standard deviation divided by the daily mean), the relative range (RR) of daily variability (difference between daily maximum and minimum divided by the daily mean), and one-day change of CV, RR, and TCO daily mean. Differences between statistical parameters of the metrics for the periods 1963–1979, 1980–1999, and 2000–2019 will be analysed to discuss the long-term changes in the metrics.

2. Materials and method

2.1. Total column ozone observations

TCO observations have been carried out at Belsk (the Central Geophysical Observatory of the Institute of Geophysics Belsk, Polish Academy of Sciences) since March 1963 using the Dobson spectrophotometer No. 84. The TCO retrieval follows the technique of the differential optical absorption spectroscopy applied to a wavelength pair with strong and weak ozone absorption in the UV range. The following pairs are used: A (305.5 and 325.0 nm), C (311.5 and 332.4 nm), and D (317.5 and 339.9 nm). Different combinations of double wavelengths pairs (AD, CD) and observation settings, direct sun (DS), zenith blue (ZB), and zenith cloudy (ZC), have been applied to achieve the highest possible accuracy of the TCO observation under given atmospheric conditions (Degórska et al., 1978).

Selection of the wavelength pairs and the observation settings follow the World Meteorological Organization (WMO) recommendations implemented in the global ozone observing network (Dobson, 1957; Komhyr, 1980). History of the ozone observations at Belsk and the instrument calibrations in the period 1963–2012 was described in our earlier publication (Krzyścin et al., 2014). Since then, another instrument calibration has taken place in Hohenpeissenberg in 2014 which confirmed the stable performance of the instrument without any signs of aging.

Numerous trend analyses were carried out using the TCO monthly means, averaging the daily representatives of TCO at Belsk, derived from manual observations by the Dobson spectrophotometer (Hill et al., 1986; Degórska et al., 1989; Bojkov et al., 1995; Krzyścin and Baranowski, 2009; Krzyścin et al., 2013). These representatives were calculated as the arithmetic mean of a few near noon observations, i.e. at least 3 for the low solar elevation season (November, December, and January) and 5 for the rest of the year, with the nominal highest quality observation. The choice of the highest quality observations depends on the solar elevation and the cloudiness type, at the moment of the observation. This criterion was adopted by WMO for the global TCO network following the recommendations of Dobson (1957) and Komhyr (1980).

The Belsk's daily TCO representatives have been archived at the World Ozone and Ultraviolet Data Centre (WOUDC) (https://woudc.org/home.php). The Dobson TCO measurements were taken throughout the day, not only around noon as recommended by WMO, up to 36 and 50 in the low and high solar elevation season, respectively. Results of all intraday TCO measurements (in total 115,736 observations during ~20,000 days in the period 23 March 1963–31 December 2019) were checked and outliers were removed. This data, divided into three subperiods (1963–1979, 1980-1999, and 2000-2019), has been stored at the PANGAEA data base (Rajewska-Więch et al., 2020) with additional information including: time of observation, description of the wavelength pairs, and observation setting for each individual measurement. Splitting the data into three subsets corresponds to three phases of the TCO long-term variability: trendless, strong decline followed by strong recovery, and finally a weak recovery (Krzyścin and Baranowski, 2019).

For comparison purposes, concurrent TCO daily values are taken from the Belsk's overpasses with Solar Backscattered UV (SBUV) instruments (1970–2019) on various satellite platforms: Nimbus 4 and 7, National Oceanic and Atmospheric Administration (NOAA) 9, 11,

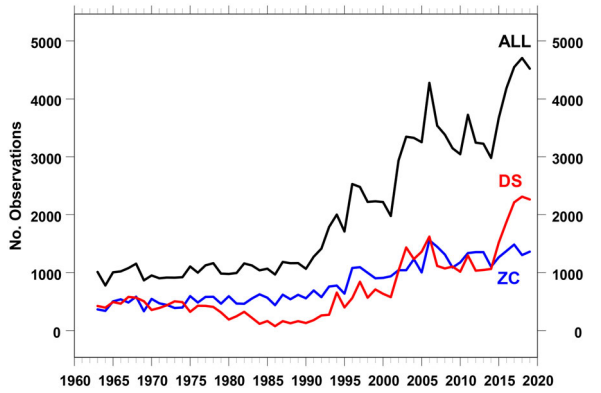

Fig. 1. Yearly number of the intraday Dobson spectrophotometer measurements in the period 1963–2019: the entire set (DS&ZB&ZC) - black curve, the DS subset – red curve, and the ZC subset – blue curve.

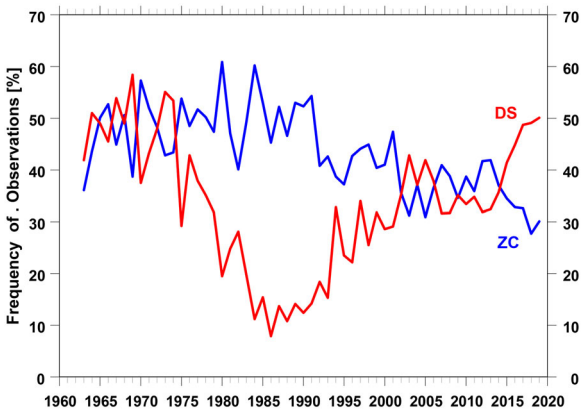

Fig. 2. The yearly frequency of the DS (red curve) and ZC (blue curve) observations in the period 1963–2019.

14, 16–19, and Suomi National Polar-orbiting Partnership (SNPP). The data are taken from SBUV Merged Ozone Data Set ver.8.6 available at https://acd-ext.gsfc.nasa.gov/Data_services/merged/.

2.2. Statistical analysis

The short-term TCO variability is discussed using metrics based on the standard statistics of the intraday TCO measurements: daily mean (*Mean*), standard deviation (*SD*), daily maximum (*Max*), and minimum (*Min*). The following intraday metrics are examined: the coefficient of variation (CV) and the relative range (RR):

$$CV = 100\% \times SD/Mean \quad (1)$$

$$RR = 100\% \times (Max - Min)/Mean \quad (2)$$

These indices are calculated for days with at least three measurements per day. Each metrics is examined in five categories of the TCO observations: the entire set, DS&ZB, AD&DS, ZC, and DS. The ranking (best to worst) of the TCO observation accuracy by the Dobson spectrophotometer is as follows: AD&DS, DS, DS&ZB, and ZC (Dobson, 1957). The subsamples of the TCO metrics are considered for statistical analyses separately for three subperiods (1963–1979, 1980–1999, and 2000–2019). Total number of TCO observations was 16,906, 29,566, and 69,264 in these subperiods, respectively.

In addition, the relative one-day change of TCO, ΔTCO_X, is used as a metrics of the interday changes of TCO:

$$\Delta TCO_X = 100\% \times \left(TCO_X(t+1) - TCO_X(t)\right)/TCO_X(t) \quad (3)$$

where $TCO_X(t+1)$ and TCO_X (t) are TCO values in two successive days, subscript "X" denotes data categories, e.g. TCO_{ALL} is for all observations, $\Delta TCO_{AD\&DS}$ for AD&DS subset, and so on. In case of TCO from SBUV Merged Ozone Data Set, the metrics is denoted as ΔTCO_{SBUV}.

Standard statistics (mean value, standard deviation, median, and 5th–95th percentile range) are calculated based on the daily values of the metrics defined by the formulas (1), (2), and (3). Moreover, the two-sample Kolmogorov–Smirnov (KS) test is applied to examine differences between statistical distributions of the metrics for three possible combinations of the data subsamples, i.e. 1963–1979 versus 1980–1999, 1963–1979 versus 2000–2019, and 1980–1999 versus 2000–2019. The two-sample KS test is a general nonparametric method for comparing two samples, based on difference in shape of the empirical cumulative distribution functions of two compared samples. This test has the advantage of analyzing cumulative distribution functions without checking the significance of differences between selected statistical parameters, such as means or medians, which requires assuming the distribution type.

3. Results

3.1. Long-term total column ozone variability

Figure 1 shows the upward trend in number of all observations per year since the early 1990s and its levelling off around 2005. This pattern reflects the growing interest in monitoring ozone at Belsk, rather than the existence of atmospheric processes that would allow more frequent observations (e.g. more sunny days). The changes in atmospheric conditions are probably imprinted mainly in the relative frequency of the ZC and DS observations (Fig. 2). The relative frequency of the DS observations looks similar at the beginning and end of the Belsk's data, i.e. in the period 1963–1979 and 2000–2019, regardless of large differences in total number of the Dobson observations totaling 16,906 and 69,264, respectively. In

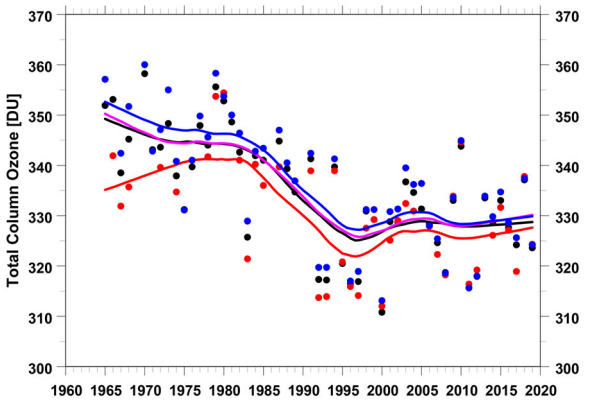

Fig. 3. The yearly means and their smoothed profile (by the lowess filter) of total column ozone taken from various subsets of the Dobson spectrophotometer measurements at Belsk in the period 1963–2019: the ZC subset (the yearly data and the smooth curve in blue), the entire set (black), the DS&ZB subset (red), and the entire set from WOUDC daily means (magenta).

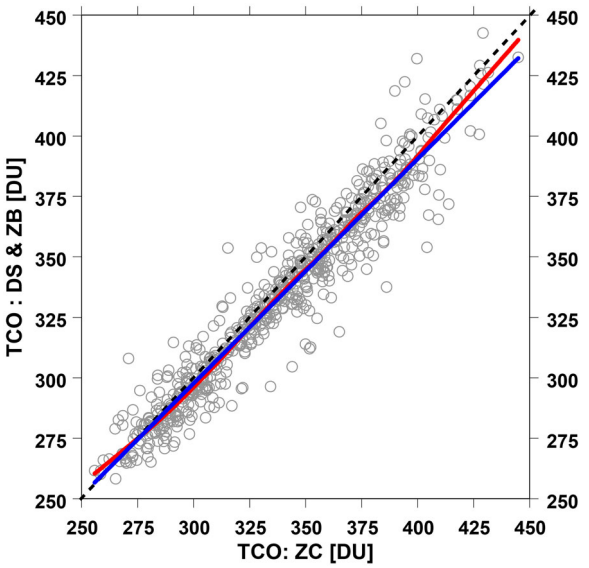

Fig. 4. The monthly means of total column ozone from the DS&ZB measurements versus the corresponding means from the ZC measurements: the linear regression fit – blue line, the smoothed curve by the lowess filter – red line, and the diagonal of the square (the perfect agreement line) – the dashed black line.

the period 1980–1999, the frequency of the DS observations was two to three times smaller when compared to the ZC observations.

Figure 3 illustrates the long-term variations of the yearly TCO means (the average of the monthly TCO means) for the period 1964–2019. Interday observations allow for calculation the time series for the entire set of the observations, and separately for different data subsets (here DS&ZB and ZC). The time series from selected subsets of TOC measurements are superposed on the time series averaging the daily TCO representatives (archived in WOUDC) calculated according to the WMO rule to average only a few high-quality observations made around noon (Dobson, 1957). There is an almost perfect correspondence between the time series averaging all available intraday observations and the daily TCO representatives. This result suggests similar results from trend analyzes based on these time series.

The long-term TCO variability patterns (Fig. 3) from the ZC subset and the non-ZC (DS&ZB) subset look different. This is especially apparent at the beginning of the first subperiod (1963–1979). The difference between the long-term ZC and non-ZC patterns (blue and red curves in Fig. 3, respectively) decreases with increasing number of the Dobson observations and equals less than ~1% at the end of the time series. There are two sources of the differences between these long-term patterns. The first is related to the basic technical differences between the Dobson's observations (DS, ZB, and ZC) and the second is related to influence of weather on monthly averages.

For several days a month, there were no DS and ZB observations due to the cloud cover. In this case, the monthly means used different numbers of the daily means. The increasing frequency of observations also means more daily values to be used in the monthly averaging, resulting in better consistency between the long-term ZC and non-ZC (DS&ZB) profiles.

The correlation coefficient between the TCO monthly means based on DS&ZB and ZC observations is 0.96 and the regression line of the DS&ZB on the ZC monthly means is $Y = 0.93\ X + 0.01$ (Fig. 4). A high agreement between these two classes exists throughout the TCO variability range because the regression line is close to a locally smoothed curve (by the lowess smoother, Cleveland, 1979).

3.2. Intraday metrics of the short-term variability of total column ozone

Table 1 shows the basic statistical parameters of TCO intraday variability for three subperiods (1963–1979, 1980–1999, and 2000–2019) including: mean value, standard deviation, and difference between the daily maximum and minimum. The mean values are in the range of ~330–345 Dobson Unit (DU), standard deviations in the range of ~4–5.5 DU, and the max–min difference in the range of ~11–17 DU. The smallest variability corresponds to the most accurate (DS&AD) class of the Dobson measurements.

The statistical parameters of CV and RR are presented in Tables 2 and 3, respectively. Mean and median of CV values are ~1–1.7%, standard deviations ~0.7–0.9%, and

Table 1. Statistical characteristics of intraday TCO variability: Mean value (Mean), standard deviation (SD), and Span (difference between the daily maximum and minimum TCO value).

Class	Mean (DU)	SD (DU)	Span (DU)	*N*
		1963–1978		
ALL	342	5.15	13.1	3551
DS&ZB	335	4.58	11.8	1661
AD&DS	334	4.48	11.4	1346
ZC	346	5.43	13.2	1366
DS	334	4.53	11.6	1420
		1980–1999		
ALL	332	4.89	13.1	5182
DS&ZB	330	4.30	11.7	2430
AD&DS	333	3.88	10.4	852
ZC	330	5.07	12.8	2464
DS	331	3.92	10.5	984
		2000–2019		
ALL	328	5.40	16.9	6440
DS&ZB	328	4.65	14.9	3782
AD&DS	330	3.69	10.7	2537
ZC	329	5.19	14.3	4068
DS	329	3.98	12.1	2891

All values are in Dobson units (DU). DS, ZB, and ZC denote direct sun, zenith blue, and zenith cloudy class of the Dobson spectrophotometer observations, respectively. AD means the observation class (with the highest accuracy) using the double wavelength pairs: A (305.5 nm, 325.0 nm) and D (317.5 nm, 339.9 nm). *N* is total number of the daily values used in the calculations for each class.

the 5th–95th percentile range ∼2–3%. The respective values for RR are ∼3–5%, 2–2.5%, and 6–8%. The largest difference between statistical values for the subperiod pairs is obtained for RR when comparing the entire data set for the 1963–1979 and 2000–2019 period, i.e. the difference is of ∼1.3 percentage point (PP), for the mean and median (see Table 3 for RR equal to 3.85% and 5.16%), and the corresponding change of ∼1.7 PP for the 5th–95th percentile range.

Table 4 shows the probabilities (using the two-sample KS test) of a hypothesis with a similar distribution of metric values in the subperiod pairs, i.e. 1963–1979 versus 1980–1999, 1963–1979 versus 2000–2019, and 1980–1999 versus 2000–2019. The distributions are mostly different as there exists a probability of less than 1% in 19 cases out of a total of 30 cases (∼63%), whereas the probability of less than 5% occurs in 70% of all cases. For the ZC subset, a hypothesis of the same distributions is rejected three times (50% possible cases). For other combination of observation types and subperiod pair, there are two cases (DS and AD&DS) with two insignificant differences (out of six cases).

Table 2. Statistical characteristics of the coefficient of variation, according formula (1), of the intraday TCO values.

Class	Mean ± SD %	Median [Range] %
	1963-1979	
ALL	1.52 ± 0.84	1.38 [0.41, 3.04]
DS&ZB	1.38 ± 0.78	1.25 [0.34, 2.80]
AD&DS	1.34 ± 0.77	1.22 [0.32, 2.74]
ZC	1.59 ± 0.91	1.44 [0.43, 3.27]
DS	1.36 ± 0.77	1.23 [0.32, 2.74]
	1980-1999	
ALL	1.48 ± 0.82	1.35 [0.41, 3.00]
DS&ZB	1.31 ± 0.74	1.20 [0.34, 2.64]
AD&DS	1.16 ± 0.73	1.00 [0.31, 2.49]
ZC	1.54 ± 0.90	1.39 [0.39, 3.22]
DS	1.18 ± 0.72	1.05 [0.32, 2.51]
	2000-2019	
ALL	1.65 ± 0.81	1.51 [0.58, 3.14]
DS&ZB	1.42 ± 0.71	1.31 [0.43, 2.73]
AD&DS	1.11 ± 0.72	0.96 [0.25, 2.41]
ZC	1.58 ± 0.89	1.43 [0.42, 3.26]
DS	1.20 ± 0.72	1.05 [0.32, 2.58]

Mean, SD, median, and [range] denote average value, standard deviation, median, and the 5th–95th percentile range. All values are percentages.

Table 3. The same as Table 2 but for the relative range of the intraday variability according formula (2).

Class	Mean ± SD %	Median [Range] %
	1963–1979	
ALL	3.85 ± 2.14	3.52 [0.98, 7.69]
DS&ZB	3.51 ± 2.02	3.17 [0.81, 7.40]
AD&DS	3.41 ± 1.98	3.09 [0.78, 7.18]
ZC	3.87 ± 2.24	3.53 [1.01, 7.99]
DS	3.46 ± 1.99	3.13 [0.79, 7.27]
	1980–1999	
ALL	3.97 ± 2.18	3.63 [1.03, 8.06]
DS&ZB	3.57 ± 2.05	3.29 [0.85, 7.35]
AD&DS	3.11 ± 1.95	2.77 [0.73, 6.56]
ZC	3.90 ± 2.29	3.53 [0.93, 8.26]
DS	3.17 ± 1.97	2.82 [0.76, 6.76]
	2000–2019	
ALL	5.16 ± 2.56	4.84 [1.54, 9.94]
DS&ZB	4.55 ± 2.40	4.26 [1.12, 8.84]
AD&DS	3.20 ± 2.12	2.78 [0.61, 7.29]
ZC	4.34 ± 2.51	3.96 [1.08, 9.05]
DS	3.65 ± 2.26	3.25 [0.79, 7.95]

3.3. One-day changes of total column ozone variability

Tables 5 and 6 show statistical parameters of the one-day changes of the metrics describing the TCO variability over the day, i.e. differences between next day and current value of CV (Table 5) and RR (Table 6). Mean and

Table 4. Probability of the same distribution for the intraday metrics in the subperiod pairs by the two-sample Kolmogorov–Smirnov test.

Variable	1963–1979 versus 1980–1999	1963–1979 versus 2000–2019	1980–1999 versus 2000–2019
		ALL	
CV	0.05	<0.01*	<0.01*
RR	0.01*	<0.01*	<0.01*
		DS&ZB	
CV	<0.01*	<0.01*	<0.01*
RR	0.20	<0.01*	<0.01*
		AD&DS	
CV	<0.01*	<0.01*	0.06
RR	<0.01*	<0.01*	0.12
		ZC	
CV	0.25	0.68	0.04*
RR	0.78	<0.01*	<0.01*
		DS	
CV	<0.01*	<0.01*	0.39
RR	<0.01*	0.13	<0.01*

The results are for the entire set of observation (ALL) and various combinations of the Dobson spectrophotometer settings (DS&ZB, AD&DS, ZC, and DS).
(…)* marks cases with the probability less than 0.05.
CV, coefficient of variability; RR, relative range.

Table 5. Statistical characteristics of one-day change of the coefficient variability.

Class	Mean ± SD PP	Median [Range] PP	*N*
		1963–1979	
ALL	0.02 ± 1.09	−0.01 [−1.82, 1.81]	2458
DS&ZB	0.03 ± 1.01	0.02 [−1.56, 1.75]	793
AD&DS	0.03 ± 0.98	0.02 [−1.59, 1.73]	629
ZC	0.06 ± 1.17	0.01 [−1.89, 1.99]	443
DS	0.02 ± 0.98	0.02 [−1.59, 1.70]	668
		1980–1999	
ALL	0.00 ± 1.11	−0.01 [−1.76, 1.87]	4108
DS&ZB	0.02 ± 0.96	0.01 [−1.57, 1.50]	1308
AD&DS	−0.01 ± 0.87	0.02 [−1.53, 1.30]	363
ZC	−0.01 ± 1.26	−0.03 [−2.11, 2.13]	1135
DS	0.01 ± 0.93	0.02 [−1.59, 1.49]	403
		2000–2019	
ALL	−0.00 ± 1.06	0.00 [−1.71, 1.69]	5857
DS&ZB	0.01 ± 0.92	0.00 [−1.45, 1.43]	2547
AD&DS	0.02 ± 0.94	0.00 [−1.44, 1.55]	1517
ZC	−0.01 ± 1.18	0.01 [−1.94, 2.01]	2528
DS	0.02 ± 0.95	0.00 [−1.46, 1.58]	1723

The same notation as in Table 2. The values are in percentage points (PP). *N* is total number of the daily values of the metrics used in the calculations for each class.

median of the differences are close to zero (between −0.03 and 0.06 PP for CV and between −0.06 and 0.16 PP for RR), whereas standard deviations are ∼1 PP and 2.5–3 PP, respectively. The 5th–95th range for one-day CV changes is ∼3.5 PP for the entire set of the observations, ∼4 PP for the ZC, and ∼3 PP for non-ZC class. The corresponding ranges for the one-day RR changes are ∼9–11 PP, 9–11 PP, and 8–10 PP.

Table 7 presents the statistical parameters of the relative one-day changes of TCO calculated using formula (3). Mean and median are close to zero both using the Dobson measurements and SBUV overpasses i.e. between −0.5% and 0.2%. Standard deviation varies from 4.3% (for AD&DS subset) up to 8.5% (for ZC subset). Standard deviation from the SBUV data is between these values, i.e. ∼ 7%. The 5th–95th percentile span is from ∼11–15% (DS subset) up to ∼26% (ZC subset). The span from the SBUV data is ∼21%.

Table 8 shows the results of the two-sample KS tests regarding the significance of differences between the samples of the one-day change of the metrics in the following subperiods: 1963–1979 versus 1980–1999, 1963–1979 versus 2000–2019, and 1980–1999 versus 2000–2019. The statistically significant differences between samples are found only in two cases out of total 30 cases (∼7%) for the CV and RR metrics, i.e. for one-day changes of RR when comparing the first and last subperiod for the entire set of the observations and for the ZC subset. For the former case, the standard deviation of one-day changes of RR increases from 2.82 PP to 3.30 PP, and the 5^{th}-95^{th} range from 9.43 PP to 10.8 PP (Table 6). For the latter case (ZC class), the corresponding values change from 2.95 PP to 3.35PP, and from 9.30 PP to 11.1 PP, respectively.

A marginally statistically significant difference (with probability ∼0.05) is found in the comparison of one-day changes of CV between the 1980–1999 and 2000–2019 subperiods using the entire sample of measurements. In this case, standard deviation decreases from 1.11 PP to 1.06 PP, and the 5th–95th range decreases from 3.63 PP to 3.4 PP (Table 5).

The two-sample KS test applied to the relative one-day change of TCO (see Table 8 for ΔTCO_X variables) shows significant difference between samples for only two cases (out of total 15 cases), when the sample from 1963 to 1979 containing all available Dobson measurements was compared with the sample from 1980–1999 to 2000–2019. The SBUV samples of one-day change of TCO have insignificant differences in the comparisons of three subperiod pairs, 1963–1979 & 1980–1999, 1963–1979 & 2000–2019, and 1980–1999 & 2000-2019.

4. Discussion and conclusions

Nowadays, increasing variability of the climate, which is possibly related to the anthropogenic forcing in recent

Table 6. The same as Table 2 but for the one-day change of the relative range that is expressed in percentage point (PP).

Class	Mean ± SD PP	Median [Range] PP	*N*
	1963-1979		
ALL	0.05 ± 2.82	0.04 [−4.71, 4.72]	2458
DS&ZB	0.05 ± 2.62	0.03 [−4.36, 4.41]	793
AD&DS	0.04 ± 2.51	0.05 [−4.17, 4.35]	629
ZC	0.16 ± 2.95	0.02 [−4.47, 4.83]	443
DS.	0.04 ± 2.54	0.03 [−4.14, 4.26]	668
	1980–1999		
ALL	−0.01 ± 2.96	0.01 [−4.80, 4.84]	4108
DS&ZB	0.06 ± 2.70	0.03 [−4.29, 4.26]	1308
AD&DS	−0.05 ± 2.43	0.02 [−4.18, 3.79]	363
ZC	−0.02 ± 3.21	−0.06 [−5.46, 5.36]	1135
DS.	0.01 ± 2.63	0.02 [−4.50, 4.01]	403
	2000–2019		
ALL	−0.01 ± 3.30	−0.01 [−5.40, 5.40]	5857
DS&ZB	0.02 ± 3.07	−0.01 [−4.97, 4.88]	2547
AD&DS	0.06 ± 2.75	0.00 [−4.33, 4.54]	1517
ZC	−0.01 ± 3.35	0.07 [−5.48, 5.65]	2528
DS	0.06 ± 2.96	0.02 [−4.83, 4.82]	1723

N is total number of the daily values of the metrics used in the calculations for each class.

Table 7. The same as Table 2 but for the relative one-day change of TCO according formula (3).

Variable	Mean ± SD %	Median [Range] %	*N*
	1963–1979		
$\Delta TCO_{\mathrm{ALL}}$	−0.4 ± 6.4	−0.4 [−11.1, 9.9]	2458
$\Delta TCO_{\mathrm{DS\&ZB}}$	−0.4 ± 4.5	−0.2 [−7.7, 6.3]	793
$\Delta TCO_{\mathrm{AD\&DS}}$	−0.3 ± 4.3	0.0 [−7.5, 6.0]	629
ΔTCO_{ZC}	−0.2 ± 8.3	−0.4 [−14.1,12.5]	443
ΔTCO_{DS}	−0.2 ± 4.5	0.0 [−5.4, 6.6]	668
$\Delta TCO_{\mathrm{SBUV}}$	0.2 ± 6.8	0.0 [−9.9, 10.6]	688
	1980-1999		
$\Delta TCO_{\mathrm{ALL}}$	−0.4 ± 6.8	−0.2 [−11.9, 11.0]	4108
$\Delta TCO_{\mathrm{DS\&ZB}}$	−0.5 ± 5.0	−0.4 [−10.0, 8.1]	1308
$\Delta TCO_{\mathrm{AD\&DS}}$	−0.5 ± 3.8	−0.4 [−8.7, 5.1]	363
ΔTCO_{ZC}	−0.4 ± 8.5	−0.1 [−13.7, 12.6]	1135
ΔTCO_{DS}	−0.5 ± 4.2	−0.4 [−6.4, 5.8]	403
$\Delta TCO_{\mathrm{SBUV}}$	0.2 ± 6.6	0.0 [−9.6, 11.0]	6278
	2000-2019		
$\Delta TCO_{\mathrm{ALL}}$	−0.3 ± 7.5	−0.1 [−13.0, 10.9]	5857
$\Delta TCO_{\mathrm{DS\&ZB}}$	−0.6 ± 5.5	−0.4 [−10.0, 8.1]	2547
$\Delta TCO_{\mathrm{AD\&DS}}$	−0.6 ± 4.6	−0.4 [−8.3, 6.5]	1517
ΔTCO_{ZC}	0.1 ± 8.2	−0.1 [−14.6, 12.0]	2528
ΔTCO_{DS}	−0.5 ± 4.8	−0.4 [−8.6, 7.6]	1723
$\Delta TCO_{\mathrm{SBUV}}$	0.2 ± 7.0	0.0 [−10.4, 11.9]	7108

The values are in percentages. *N* is total number of the daily values of the metrics used in the calculations for each class.

decades, is a widely discussed issue (Nicholls and Alexander, 2007; Fischer and Knutti, 2015; Baker et al., 2018). The comparisons of the intraday values of the metrics between the 1963–1979/1980–1999/2000–2019/subperiods reveal changes of the intraday TCO variability for many classes of the TCO observations (in 21 cases out of a total 30 cases, Table 4). This is also confirmed in Fig. 5, which shows that an increasing trend began around 1985. However, the number of the intraday manual observations is also increasing (Fig. 1) due to the growing interest in the ozone variability after discovery of the ozone hole in 1983 (Chubachi, 1984). Larger span of the observed intraday TCO values could be supposed as the data extremes within the day could be better identified by frequent sampling.

The two-sample KS test applied to the intraday (next day minus current day value) changes of the metrics also reveal a change in the short-term TCO variability but for a limited number of cases (4 cases out of total 48, Table 8). The sample size increased from 2458 int the first subperiod, to 4108 in the middle subperiod to reach 5877 in the last subperiod for the entire class of the observations (Table 5). The differences between the distribution of interday metrics are always found to be statistically insignificant when comparing the samples for the 1980–1999 and 2000–2019 subperiods (last column in Table 8), despite the larger size of the latter subset. Moreover, the analysis shows insignificant differences after comparing satellite data taken from the SBUV Merged Ozone Dataset.

A statistically significant change is revealed by the comparison of one-day changes in RR between the 1963–1979 and 2000–2019 subset for the entire set of observations and for the ZC subset (Table 8). However, in these cases, standard deviation and the 5th–95th percentile range increased only slightly (Table 6). Another two cases with statistically significant change between subsamples are identified for the relative one-day change of TCO for the entire set of measurements, when the 1963–1979 sample is compared with the 1980–1999 and 2000–2019 sample.

Therefore, this analysis does not categorically confirm an increase of the variability of the short-term (with time scale up to one-day) fluctuations in TCO at Belsk. The observed significant increase in the variability of the intraday metrics of the TCO fluctuations is probably strongly affected by increasing frequency of the ozone observations at Belsk.

TCO measurements are of the highest quality when using the AD double wavelength pairs for DS measurements (Komhyr, 1980). TCO values from ZC observations are less reliable as not directly calculated from the ratio between the measured intensity of the UV radiation at two wavelengths, weakly and strongly absorbed by ozone. In this case, the empirical corrections to the ratio between UV irradiances were applied that depended on

Table 8. Probability of the same distribution for the one-day change of the intraday metrics (CV, RR, and ΔTCO_X) in the subperiod pairs by the two-sample Kolmogorov–Smirnov test applied to the entire set of the Dobson measurements and various combinations of the instrument settings.

Variable	1963–1979 versus 1980–1999	1963–1979 versus 2000–2019	1980–1999 versus 2000–2019
	ALL		
ΔCV	0.80	0.09	0.05
ΔRR	0.32	<0.01*	0.18
ΔTCO_{ALL}	<0.01*	<0.01*	0.78
ΔTCO_{SBUV}	0.92	0.92	0.62
	DS&ZB		
ΔCV	0.90	0.43	0.55
ΔRR	0.60	0.13	0.20
$\Delta TCO_{DS\&ZB}$	0.19	0.10	0.99
	AD&DS		
ΔCV	0.47	0.69	0.78
ΔRR	0.85	0.24	0.45
$\Delta TCO_{AD\&DS}$	0.14	0.22	0.16
	ZC		
ΔCV	0.33	0.53	0.51
ΔRR	0.13	0.04*	0.65
ΔTCO_{ZC}	0.98	0.80	0.80
	DS		
ΔCV	0.85	0.76	0.99
ΔRR	0.91	0.10	0.34
ΔTCO_{DS}	0.27	0.21	0.29

ΔTCO_{SBUV} shows the probability based on the comparisons of the satellite data over Belsk (SBUV Merged Ozone Data Set).
*Marks cases with the probability less than 0.05.
$\Delta CV = CV(t+1) - CV(t)$, one-day change of CV in PP.
$\Delta RR = RR(t+1) - RR(t)$, one-day change of RR in PP.
ΔTCO_X, relative one-day change of TCO for subset X in %.

cloudiness type (Rindert, 1973; Degórska et al., 1978). It seems impossible to account for a wide range of cloud variability at the measuring site when calculating ozone. However, there were small differences between the metrics of the TCO intraday fluctuations for the most accurate AD&DS subset and the least accurate ZC subset. For CV and RR metric of the intraday variability derived from the ZC subset, the 5th–95th ranges were larger of ~0.4–0.7 PP (Table 2) and ~ 0.6–1.5 PP (Table 3) when compared with corresponding values from AD&DS observations, respectively.

The DS&ZB observations are not always possible at Belsk because of numerous cloudy days. The long-term variability of TCO derived only from the DS&ZB subset of observations showed agreement with the long-term pattern based on the entire data sets but it was worse in the period with a limited number of the Dobson observations (Fig. 3). Moreover, there was a different proportion

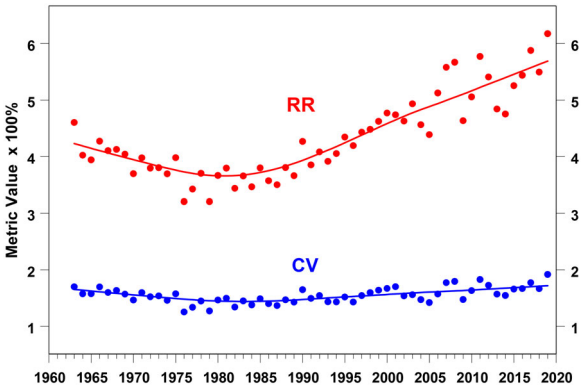

Fig. 5. The yearly means (1963–2019) and their smoothed pattern derived from the daily values of the intraday metrics of the short-term total column ozone variability: coefficient of variability (blue) and the relative range (red).

between the number of the non-cloudy (DS&ZB) and cloudy day (ZC) observations, depending to some extent on the observation policy. The number of the DS&ZB daily means were 1.22 larger than the ZC daily means in the period 1963–1979. Whereas, the rate was 0.99 and 0.93 for the period 1980–1999 and 2000–2019, respectively (see N values in Table 1).

Cloudless or overcast conditions over Belsk are related to specific air masses advection over the observing site. For example, cloudless days appear frequently during advection of the cold air from the north and north/east in winter and highly variable cloudiness appears during advection of the wet Atlantic air masses in summer. Therefore, the monthly TCO averages should include the whole spectrum of the atmospheric masses appearing over the site.

Envisaged limitation of the manual TCO observations to only ones with the highest accuracy rank, because of expected diminished interest in the ozone monitoring in the trendless era of the stratospheric ozone, which seems to begin at Belsk in the early 2000s (Fig. 3), will lead to an underestimation of the TCO variability in all time scales from the short-term (~1 day) up to the long-term ones (~10 yr.). This problem also concerns the Dobson stations operating in the northernmost part of the mid-latitudinal zone with abrupt changes of the weather conditions and many cloudy days. In such circumstances, observers will focus on the DS&ZB observations near local noon avoiding less reliable ZC observations. Therefore, the monthly means will not represent the "true" means when future data collection policy is driven by funding constrains restricting TCO measurements to perfect weather days only.

The main findings of the paper are summarized as follows:

- assumption of the constant TCO value throughout the day is frequently invalid
- the short-term TCO variability (with time scale up to ~1 day) changed only slightly (if ever) since the beginning of the ozone observations at Belsk
- for trend estimates, all types of the ozone observations should be carried out in higher latitude stations, not only these with the higher accuracy rank

It is expected, that the intraday TCO data base will be very useful when new ozone absorption coefficients are officially recommended by WMO for the global network of the ozone monitoring as expected from recent papers (Redondas et al., 2014; Wang et al., 2019). In such circumstances the revaluation of the previous TCO values (based on the Bass-Pour absorption coefficients for a fixed temperature, Bass and Paur, 1985; Komhyr et al., 1993) will be necessary. The correction coefficient to be applied for the WOUDC data should be derived taking into account all types of the ozone observations not only to the AD&DS subset.

Acknowledgements

This work was supported by the Ministry of Science and Higher Education of Poland under Grant number 3841/E-41/S/2020; and the Chief Inspectorate of Environmental Protection, Poland under Grant number GIOŚ/19/2021/DMŚ/NFOŚ.

Disclosure statement

No potential conflict of interest was reported by the authors

Funding

This work was supported by the Ministry of Science and Higher Education of Poland under Grant number 3841/E-41/S/2020; and the Chief Inspectorate of Environmental Protection, Poland under Grant number GIOŚ/19/2021/DMŚ/NFOŚ.

Data availability statement

The dataset used in this article is available on the PANGAEA repository (Rajewska-Więch et al., 2020, https://doi.org/10.1594/PANGAEA.919378).

References

Baker, H. S., Millar, R. J., Karoly, D. J., Beyerle, U., Guillod, B. P. and co-authors. 2018. Higher CO_2 concentrations increase extreme event risk in a 1.5 °C world. *Nat. Clim. Change* **8**, 604–608. doi:10.1038/s41558-018-0190-1

Ball, W. T., Alsing, J., Mortlock, D. J., Staehelin, J., Haigh, J. D.and co-authors. 2018. Evidence for a continuous decline in lower stratospheric ozone offsetting ozone layer recovery. *Atmos. Chem. Phys.* **18**, 1379–1394. doi:10.5194/acp-18-1379-2018

Bass, A. M. and Paur, R. J. 1985. The ultraviolet cross-sections of ozone: I. The measurements. In: *Atmospheric Ozone* (eds. C.S. Zerefos and A. Ghazi). Springer, Dordrecht. pp. 606–610.

Bojkov, R., Bishop, L. and Fioletov, V. E. 1995. Total ozone trends from quality-controlled ground-based data (1964–1994). *J. Geophys. Res.* **100**, 25867. doi:10.1029/95JD02907

Chipperfield, M. P., Dhomse, S., Hossaini, R., Feng, W., Santee, M. L.and co-authors. 2018. On the cause of recent variations in lower stratospheric ozone. *Geophys. Res. Lett.* **45**, 5718–5726. doi:10.1029/2018GL078071

Chubachi, S. 1984. Preliminary result of ozone observations at Syowa from February 1982 to January 1983. *Mem. Natl Inst. Polar Res.* **34**, 13–19.

Cleveland, W. S. 1979. Robust weighted regression and smoothing scatterplots. *J. Am. Stat. Assoc.* **74**, 829–836. doi:10.1080/01621459.1979.10481038

Crutzen, P. J. 1971. Ozone production rates in an oxygen-hydrogen-nitrogen oxide atmosphere. *J. Geophys. Res.* **76**, 7311–7327. doi:10.1029/JC076i030p07311

Dobson, G. M. B. 1957. Observers' handbook for the ozone spectrophotometer. *Ann. IGY* **5**, 46–89.

Degórska, M., Rajewska-Więch, B. and Kowalczyk, R. 1978. A program for computing routine total ozone measurements and lamp tests for a Dobson spectrophotometer. *Publ. Inst. Geophys. Pol. Acad. Sci.* **D-7**, 67–75.

Degórska, M., Krzyścin, J. and Rajewska-Więch, B. 1989. Ozone trends from Dobson station at Belsk, Poland. In: *Proceedings of the Quadrennial Ozone Symposium 1988 and Tropospheric Ozone Workshop*, Göttingen, FRG. Hampton, VA, A. Deepak Publishing, 120–123.

Dhomse, S. S., Kinnison, D., Chipperfield, M. P., Salawitch, R. J., Cionni, I.and co-authors. 2018. Estimates of ozone return dates from Chemistry-Climate Model Initiative simulations. *Atmos. Chem. Phys.* **18**, 8409–8438. doi:10.5194/acp-18-8409-2018

Farman, J. C., Gardiner, B. G. and Shanklin, J. D. 1985. Large losses of total ozone in Antarctica reveal seasonal ClOx/NOx interaction. *Nature* **315**, 207–210. doi:10.1038/315207a0

Fischer, E. and Knutti, R. 2015. Anthropogenic contribution to global occurrence of heavy-precipitation and high-temperature extremes. *Nature Clim. Change* **5**, 560–564. doi:10.1038/nclimate2617

Harris, N. R. P., Kyrö, E., Staehelin, J., Brunner, D., Andersen, S.-B.and co-authors. 2008. Ozone trends at northern mid- and high latitudes – a European perspective. *Ann. Geophys.* **26**, 1207–1220. doi:10.5194/angeo-26-1207-2008

Hill, W. J., Oehlert, G. W. and Reinsel, G. C. 1986. Trend analysis sensitivity studies of Dobson total ozone data

through 1984. *J. Geophys. Res.* **91**, 14515. doi:10.1029/JD091iD13p14515

Komhyr, W. D. 1980. *Operations handbook – ozone observations with a Dobson spectrophotometer.* WMO Global Ozone Research and Monitoring Project, Report No. 6, Geneva, Switzerland.

Komhyr, W. D., Mateer, C. L. and Hudson, R. D. 1993. Effective Bass-Paur 1985 ozone absorption coefficients for use with Dobson ozone spectrophotometers. *J. Geophys. Res.* **98**, 20451–20465. doi:10.1029/93JD00602

Komhyr, W. D., Grass, R. D. and Leonard, P. K. 1989. Dobson spectrometer 83: a standard for total ozone measurements, 1962-1987. *J. Geophys. Res.* **94**, 9847–9861. doi:10.1029/JD094iD07p09847

Krzyścin, J. W. and Rajewska-Więch, B. 2009. Ozone recovery as seen in perspective of the Dobson spectrophotometer measurements at Belsk (52°N, 21°E) in the period 1963–2008. *Atmos. Environ.* **43**, 6369–6375. doi:10.1016/j.atmosenv.2009.09.018

Krzyścin, J. W., Rajewska-Więch, B. and Jarosławski, J. 2013. The long-term variability of atmospheric ozone from the 50-yr observations carried out at Belsk (51.84°N, 20.78°E), Poland. *Tellus B* **65**, 21779. doi:10.3402/tellusb.v65i0.21779

Krzyścin, J. W., Borkowski, J., Głowacka, A., Jarosławski, J., Podgórski, J. and co-authors 2014. Half century of the ozone observation at the Central geophysical Laboratory, IGF, PAS, Belsk, Poland. In: *Achievements, History and Challenges in Geophysics* (eds. R. Bialik, M. Majdański, M. Moskalik), GeoPlanet: Earth and Planetary Sciences, Springer, Cham, Switzerland, pp. 85–107.

Krzyścin, J. W. and Baranowski, D. 2019. Signs of the ozone recovery based on multi sensor reanalysis of total ozone for the period 1979–2017. *Atmos. Environ.* **199**, 334–344. doi:10.1016/j.atmosenv.2018.11.050

Krzyścin, J. 2020. Is the Antarctic ozone hole recovering faster than changing the stratospheric halogen loading? *J. Meteorologic. Soc. Jpn.* **98**, 1083–1091. doi:10.2151/jmsj.2020-055

Kuttippurath, J., Kumar, P., Nair, P. J. and Pandey, P. C. 2018. Emergence of ozone recovery evidenced by reduction in the occurrence of Antarctic ozone loss saturation, *npj. Climate Atmos. Sci.* **1**, 1–8.

Molina, M. and Rowland, F. 1974. Stratospheric sink for chlorofluoromethanes: chlorine atom-catalysed destruction of ozone. *Nature* **249**, 810–812. doi:10.1038/249810a0

Montzka, S. A., Dutton, G. S., Yu, P., Ray, E., Portmann, R. W.and co-authors. 2018. An unexpected and persistent increase in global emissions of ozone-depleting CFC-11. *Nature* **557**, 413–417. doi:10.1038/s41586-018-0106-2

Morgenstern, O., Giorgetta, M. A., Shibata, K., Eyring, V., Waugh, D. W.and co-authors. 2010. Review of the formulation of present-generation stratospheric chemistry-climate models and associated external forcings. *J. Geophys. Res.* **115**, 1–21. doi:10.1029/2009JD013728

Nicholls, N. and Alexander, L. 2007. Has the climate become more variable or extreme? Progress 1992-2006. *Prog. Phys. Geog.* **31**, 77–87. doi:10.1177/0309133307073885

Pazmiño, A., Godin-Beekmann, S., Hauchecorne, A., Claud, C., Khaykin, S.and co-authors. 2018. Multiple symptoms of total ozone recovery inside the Antarctic vortex during austral spring. *Atmos. Chem. Phys.* **18**, 7557–7572. doi:10.5194/acp-18-7557-2018

Rajewska-Więch, B., Krzyścin, J. W., Sobolewski, P. and Wink, J. 2020. Intraday total column ozone measurements at Belsk, Poland, with the Dobson spectrophotometer no.84 since March 23, 1963 up to December 31, 2019, Institute of Geophysics of the Polish Academy of Sciences, Warsaw, Poland. *PANGAEA*,.

Redondas, A., Evans, R., Stuebi, R., Köhler, U. and Weber, M. 2014. Evaluation of the use of five laboratory-determined ozone absorption cross sections in Brewer and Dobson retrieval algorithm. *Atmos. Chem. Phys.* **14**, 1635–1648. doi:10.5194/acp-14-1635-2014

Reinsel, G. C., Miller, A. J., Weatherhead, E. C., Flynn, L. E. and Nagatani, R. M. and co-authors. 2005. Trend analysis of total ozone data for turnaround and dynamical contributions. *J. Geophys. Res.* **110**, 1–14.

Rigby, M., Park, S., Saito, T., Western, L. M., Redington, A. L.and co-authors. 2019. Increase in CFC-11 emissions from eastern China based on atmospheric observations. *Nature* **569**, 546–550. doi:10.1038/s41586-019-1193-4

Rindert, S. B. 1973. *Constructing empirical blue-sky ozone charts.* Department of Meteorology, Report No.36, University of Uppsala, Uppsala, Sweden, 37pp.

Staehelin, J., Petropavlovskikh, I., De Mazière, M. and Godin-Beekmann, S. 2018. The role and performance of ground-based networks in tracking the evolution of the ozone layer. *C. R. Geosci.* **350**, 354–367. doi:10.1016/j.crte.2018.08.007

Solomon, S., Ivy, D. J., Kinnison, D., Mills, M. J., Neely, R. R.and co-authors. 2016. Emergence of healing in the Antarctic ozone layer. *Science* **353**, 269–274. doi:10.1126/science.aae0061

Wang, H., Chai, S., Tang, X., Zhou, B., Bian, J. and co-authors. 2019. Application of temperature dependent ozone absorption cross-sections in total ozone retrieval at Kunming and Hohenpeissenberg stations. *Atmos. Environ.* **215**, 116890. doi:10.1016/j.atmosenv.2019.116890

WMO (World Meteorological Organization) 2018. *Scientific Assessment of Ozone Depletion: 2018*. Global Ozone Research and Monitoring Project-Report No. 58, Geneva, Switzerland, 588pp.